International Journal of Nanomedicine

Dovepress
Taylor & Francis Group

Open Access Full Text Article

ORIGINAL RESEARCH

A New Nanocomposite for Inducing Demineralized Dentin Remineralization

Guifei Ban[1,2,*], Jindong Long[1,2,*], Kaiqi Yan[1,2,*], Qiurong Li[1,2], Xiaoman Huang[1,2], Xiaolang Wei[1,2], Fangfang Xie[1,2]

[1]College & Hospital of Stomatology, Guangxi Medical University, Nanning, Guangxi, 530021, People's Republic of China; [2]Guangxi Key Laboratory of Oral and Maxillofacial Rehabilitation and Reconstruction, College of Stomatology, Hospital of Stomatology, Guangxi Medical University, Nanning, Guangxi, China; Guangxi Health Commission Key Laboratory of Prevention and Treatment for Oral Infectious Diseases, College of Stomatology, Hospital of Stomatology, Guangxi Medical University, Nanning, Guangxi, 530021, People's Republic of China

*These authors contributed equally to this work

Correspondence: Fangfang Xie, Email xiedualfang@163.com

Objective: This study aimed to investigate a method for promoting the remineralization of demineralized dentin collagen fibers, with the objective of enhancing the bonding strength and durability of dentin resin while reducing the incidence of secondary caries.

Methods: A mineralized solution, PAMAM-COOH/ACMP-MDP ethanol solution, was prepared, consisting of the dendritic organic macromolecule PAMAM-COOH, magnesium ions, and methacryloyloxydecyl dihydrogen phosphate (MDP). We examined its storage stability. The solution underwent comprehensive characterization using various techniques, including Fourier Transform Infrared Spectroscopy (FTIR), X-Ray Diffraction (XRD), Transmission Electron Microscopy (TEM), STEM-EDX mapping, and Selected Area Electron Diffraction (SAED). Additionally, remineralization of demineralized dentin was induced by both control groups and the PAMAM-COOH/ACMP-MDP group. The effects were observed using a laser scanning confocal fluorescence microscope (CLSM), scanning electron microscopy (SEM), and TEM.

Results: The PAMAM-COOH/ACMP-MDP ethanol solution we prepared maintained stable physicochemical properties after two months of storage. It exhibited good dispersibility, retained an amorphous phase, and maintained a nanometer size with excellent stability. The results from CLSM indicated that, compared to the control group, the PAMAM-COOH/ACMP-MDP ethanol solution could induce partial remineralization of demineralized dentin in deeper dentin tubules. The SEM results indicated that the PAMAM-COOH/ACMP-MDP group exhibited distinct characteristics of collagen fiber remineralization, both on the surface and within the deep dentin tubules. The collagen fibers in this group were thicker and more mineralized. Furthermore, significant remineralization features of collagen fibers were observed in the peritubular dentin of the PAMAM-COOH/ACMP-MDP group as evidenced by TEM.

Conclusion: The PAMAM-COOH/ACMP-MDP ethanol solution exhibits thermodynamic stability, uniform dispersion, and the capability to induce remineralization of demineralized dentin collagen fibers. These findings highlight the potential of dendritic macromolecules for the biomimetic mineralization of dentin collagen and underscore the feasibility of utilizing ethanol-based primers in the development of new adhesives and their clinical applications.

Keywords: nanocomposite, dentin remineralization, polyamidoamine, collagen

Introduction

Resin filling is the primary treatment method for caries, and its longevity largely depends on the adhesion between tooth enamel and dentin and the repair materials. During dentin bonding, dentin is composed of hydroxyapatite, type I collagen fibers, and non-collagen proteins.[1] After acid etching, loose collagen fiber networks form on the surface of dentin, and the adhesive cannot entirely displace the water present within these collagen fiber networks, leading to the exposure of some collagen fibers.It is readily degraded by various enzymes in the oral cavity, which compromises the durability of dentin bonding[2,3] and contributes to the occurrence of secondary caries.[4,5] Achieving remineralization of dentin during the restoration process can significantly enhance the bond strength between resin and dentin, thereby greatly extending the

Received: 4 November 2024
Accepted: 4 January 2025
Published: 1 February 2025

lifespan of the restoration.[6] The internal mineralization of collagen fibers plays a significant role in enhancing the mechanical properties of hard tissues, which in turn determines the superior mechanical and biological characteristics of natural hard tissues.[7] The key to achieving the remineralization of dentin collagen fibers lies in promoting mineralization within these fibers.

During the process of dentin biomineralization, calcium and phosphorus are sequentially deposited in and between dentin collagen fibers under the regulation of non-collagenous proteins (NCPs), leading to the formation of hydroxyapatite (HAP) after crystallization.[8] Due to the difficulty in obtaining natural NCPs, bionic mineralization has emerged, wherein calcium and phosphorus ions are artificially induced to deposit in an orderly manner within the collagen fibers, resulting in hydroxyapatite formation. As biomimetic mineralization has progressed, researchers have discovered that various forms of metastable calcium phosphate, particularly amorphous calcium phosphate (ACP), are produced during the crystallization of calcium and phosphorus. This phenomenon is crucial for achieving mineralization within collagen fibers; however, ACP exhibits poor thermodynamic stability. In biological systems, NCPs rely on numerous COO- groups to stabilize ACP for a limited duration.[9] Several studies have employed NCP analogues, such as polyaspartic acid and polyacrylic acid, to stabilize ACP, leveraging their high fluidity and liquid properties to facilitate intrafibrous mineralization of collagen.[8,10] In vivo, NCPs are carboxyl-rich acidic proteins that can coordinate with calcium ions and provide additional nucleation sites.[11,12] Polyamidoamine (PAMAM) is a dendritic macromolecular polymer, which, when its terminal reaction groups are replaced by carboxyl groups, forms carboxylated polyamidoamine (PAMAM-COOH). Due to its richness in carboxyl groups, PAMAM-COOH may play a significant role in the biomineralization process.

Studies have demonstrated that PAMAM-COOH can penetrate collagen fibers and bind to specific sites, effectively stabilizing and decelerating the transition of HAP precursors to the crystalline state of HAP, thus exhibiting significant advantages in bionic mineralization.[13–15] PAMAM-COOH/n-HAP nanocomposites can condense with nano-hydroxyapatite (n-HAP) to form PAMAM-COOH/n-HAP nanocomposites, which adhere to dentin collagen fibers via surface carboxyl groups, promoting dentin mineralization and sealing dentin tubules.[16] Furthermore, PAMAM-COOH reacts with ACP to synthesize PAMAM-COOH/ACP nanocomplexes, which recruit ACP to specific sites within collagen fibers and facilitate its crystallization into HAP, thereby achieving mineralization within the collagen matrix.[17,18] However, the PAMAM-COOH/ACP nanocomplex exhibits poor stability, is prone to polymerization, and poses preservation challenges. Therefore, this study introduces magnesium ions, known for their stabilizing effect on ACP, into the mineralization system to enhance ACP stability, resulting in the development of a novel nanocomposite material: carboxylated polyamide-amine-stabilized amorphous calcium magnesium phosphate (PAMAM-COOH/ACMP). Additionally, as the solvent for resin adhesives is typically an ethanol solution, the insolubility of PAMAM-COOH/ACMP nanocomplexes in ethanol limits their potential for clinical application.

Methacryloyloxydecyl dihydrogen phosphate(MDP) is a crucial acid-etch monomer component found in many adhesives, characterized by both hydrophilic and lipophilic structures, and shares common properties with surfactants. The bonding mechanism between the self-bonding resin adhesive containing MDP and dentin primarily involves the release of H+ ions from its phosphate group, which demineralizes and infiltrates the dentin matrix. Once a certain depth is reached, an increase in environmental calcium and phosphorus ion concentrations, along with a rise in pH, leads to a balance between demineralization and remineralization. Consequently, MDP can react with the remaining hydroxyapatite components in dentin, facilitating the formation of chemical adhesion. Additionally, the establishment of micromechanical retention[19,20] significantly contributes to reducing collagen degradation, enhancing adhesion stability, and extending the longevity of the bond.

In this study, we synthesized a novel carboxylated polyamide-amine/amorphous calcium phosphate-decyl phosphate methacrylate nanocomplex (PAMAM-COOH/ACMP-MDP) ethanol solution mineralization system at low temperature. By utilizing the lipophilic end of MDP to enhance its fat solubility, MDP maintains a stable nanoscale size in ethanol solution over extended periods. We confirmed that the PAMAM-COOH/ACMP-MDP ethanol solution was thermodynamically stable, well-dispersed, and could be stored at room temperature for prolonged durations while retaining its original properties and size. Additionally, it possessed the fundamental characteristics required for biomimetic mineralization of resin bonding to interfacial demineralized collagen fibers in dentine. Furthermore, it could effectively induce both partially

and completely demineralized dentine collagen fibers to remineralize, achieving significant mineralization effect. These results suggested that the PAMAM-COOH/ACMP-MDP ethanol solution held considerable promise for the development of new resin adhesives, which could enhance caries treatment and prolong the service life of resin prosthetics.

Materials and Methods

Preparation of PAMAM-COOH/ACMP Ethanol Solution

The preparation of PAMAM-COOH/ACMP was conducted following our previously established method.[18] Liquid A consisted of 0.625 mm PAMAM-COOH (3rd generation, Shandong CYD, China), 9.75 mm Ca^{2+}, and 0.25 mm Mg^{2+}, all dissolved in 50 vol% ethanol. A 6 mm H_3PO_4 solution was prepared by adding 85% H_3PO_4 to the 50 vol% ethanol to yield liquid B. Both solutions were pre-cooled to 10°C and then mixed in a 1:1 volume ratio. Following a 30-minute reaction, the PAMAM-COOH/ACMP remineralized ethanol solution was filtered using a 0.22 μm needle filter.

Preparation of PAMAM-COOH/ACMP-MDP Ethanol Solution

The estimated molar ratio of MDP to PAMAM-COOH was based on our previous study,[17] a PAMAM-COOH/ACMP unit maybe consists of a central PAMAM-COOH molecule and 224 $Ca_3(PO_4)_2{\cdot}4H_2O$, the molecular structure of PAMAM-COOH/ACMP-MDP was predicted, and the end group of each PAMAM-COOH maybe connected with 8 $Ca_3(PO_4)_2{\cdot}4H_2O$ and at least 8 MDP. The predicted structure was shown in Figure S1. The preparation method for liquid A was the same as described above. A total of 19.4 mg of MDP was added to 10 mL of 50% ethanol, followed by ultrasonication and vortex mixing. Then, 4.10 μL of 85% phosphoric acid was added, and the mixture was vortexed to form liquid B, which was subsequently stored at 4°C. Both solutions were vortex mixed in 5 mL aliquots and placed in a shaker at 10°C for a continued reaction lasting 30 minutes, after which they were stored at 4°C.

Characterization and Storage Stability Testing of PAMAM-COOH/ACMP and PAMAM-COOH/ACMP-MDP

After preparing the PAMAM-COOH/ACMP remineralized solution and PAMAM-COOH/ACMP-MDP, immediate testing was conducted. Fourier Transform Infrared Spectroscopy (FTIR) was employed to obtain information on the chemical structure, X-Ray Diffraction (XRD) was utilized to gather phase information, Transmission Electron Microscopy (TEM) was used to observe particle size and morphological characteristics, element distribution was assessed using STEM-EDX mapping, and Selected Area Electron Diffraction (SAED) was applied to evaluate phase characteristics. For particle size analysis via TEM, five random fields from each material sample were examined, and eight particles were randomly selected from each field to measure their diameters, with each particle measured three times to obtain an average value. The average particle diameter and standard deviation were presented as X±S. Furthermore, after storing the remineralization solution for 60 days, all tests were repeated.

Preparation of ACMP

ACMP was prepared following the method described by Gelli et al.[21] $MgCl_2$ and $CaCl_2$ were dissolved in deionized water to achieve concentrations of 8 mm for Ca^{2+} and 2 mm for Mg^{2+}. Additionally, NaH_2PO_4 was dissolved in deionized water to a concentration of 6 mm. The two solutions were mixed in a 1:1 volume ratio and stirred using a magnetic stirrer. After adjusting the pH to 7.0 with 1 M NaOH, the mixture was allowed to react for 15 minutes. The solution was then centrifuged in a tube equipped with a 0.22 μm microporous filter membrane (4°C, 10,000 rpm, for 5 minutes), and the precipitate was collected. The precipitate was washed twice with anhydrous ethanol and subsequently collected for freeze-drying, resulting in a white powder of ACMP, which was stored for future use.

Preparation of Fluorescently Labeled Materials

Calcium derived from calcium chlorophyll was utilized as a labeling agent in this experiment. Initially, $CaCl_2$ was dissolved in deionized water to create a 50 mm $CaCl_2$ aqueous solution. Subsequently, an excess of calcium chlorophyll was added to this solution, and any surplus calcium chlorophyll was removed by filtering through a 0.22 μm syringe

filter, resulting in a fluorescently labeled 50 mm $CaCl_2$ aqueous solution. The preparation follows the methodology for the non-fluorescently labeled remineralization solution. Ultimately, fluorescently labeled ACMP, PAMAM-COOH/ACMP, and PAMAM-COOH/ACMP-MDP remineralization solutions were obtained.

Preparation of Human Dentin Tablet

Approved by the Ethics Committee of Guangxi Medical University (Approval No. 2022–0026) and after obtaining informed consent from the patients, fresh extracted third molars (free of caries, defects, or white spots) were collected from the Affiliated Stomatological Hospital of Guangxi Medical University. The soft tissue on the surfaces was excised using a scalpel, and the samples were embedded and fixed in epoxy resin. A hard tissue microtome was then used to cut the dentin portion into tablets with dimensions of 3mm × 3mm × 1mm, followed by sequential polishing with water sandpaper and ultrasonic cleaning. Some dentin testing procedures require that the sample be free of minerals, such as TEM. According to our previous study,[17] the dentin tablets were immersed in a 0.5 mol/L EDTA solution at pH 7 and demineralized in a shaking incubator at 37°C for 14 days, then treated with a 1 mmol/L NaCl solution and ultrasonic cleaning to remove non-collagen proteins and any residual minerals and EDTA. This process resulted in a completely demineralized dentin. After preparation, one tablet was randomly selected for TEM observation to assess the presence of any residual mineral tissue. The complete demineralized dentin tablet was shown in Figure S2, no obvious deeply stained mineral residue was found.

For the untreated dentin tablets, they were treated with 37% phosphoric acid for 15 seconds, rinsed with deionized water for 30 seconds, and subjected to ultrasonic agitation to obtain a partially demineralized dentin, which was subsequently stored in deionized water for future use.

Remineralization of the Partial Demineralized Dentin

The experiments were grouped according to the mineralization solution. Group A(Blank group, 50% ethanol), Group B (ACMP group, 50% ethanol with added ACMP at a concentration of 3 mg/mL). Group C(MDP group, MDP solid dissolved in 50% anhydrous ethanol at a concentration of 3 mm, filtered through a 0.22 μm syringe filter for later use). Group D(PAMAM-COOH/ACMP remineralization solution). Group E(PAMAM-COOH/ACMP-MDP remineralization solution).

According to the aforementioned groups, five dentin specimens were prepared for each group, with each specimen immersed in 0.5 mL of the fluorescently labeled solution corresponding to its respective group. Following a 7-day incubation at 37°C in a constant temperature incubator with 100% humidity and protection from light, the dentin specimens were removed, rinsed with deionized water for 30 seconds, and stored in deionized water for measurement. The surface longitudinal sections of the dentin specimens were examined using a laser scanning confocal fluorescence microscope (CLSM). In each group, five random longitudinal sections of dentin were selected for high-magnification observation (×1000) within the CLSM interface. For each field of view, eight random dentinal tubules were selected to measure the depth of fluorescent labeling penetration, with each tubule measured three times to obtain an average value. The statistical results of the penetration depth of dentinal tubules in each group were presented as $x \pm S$.

Remineralization of Complete Demineralized Dentin

According to the described grouping, each group consisted of five dentin slices, with each slice immersed in 0.5 mL of the corresponding solution, which has been filtered through a 0.22 μm syringe filter. After a 7-day incubation period in a constant temperature chamber at 37°C and 100% humidity, the dentin slices were removed, rinsed in deionized water for 30 seconds, and stored in deionized water until testing. SEM and TEM analyses were performed. For SEM analysis, after removal from deionized water, the dentin underwent a gradient dehydration process, critical point drying, and gold sputtering. The surface morphology of human dentin collagen fibers was then observed using a scanning electron microscope at an accelerating voltage of 5 kV. For TEM analysis, the dentin slices were immersed in an electron microscope fixative and kept in the dark at room temperature for 2 hours, after which they were transferred to 4°C for dark storage. The slices were subsequently cut in half for longitudinal sectioning to prepare ultra-thin slices, which were examined for remineralization of human dentin collagen fibers at an accelerating voltage of 80 kV.

Statistical Analysis

The statistical analysis was performed using SPSS 22.0 software. A *T*-test was employed to compare the average particle sizes of the two materials. A paired *T*-test was utilized to compare the average particle size of each material when newly prepared versus after being stored for 60 days. For the comparison of average fluorescence penetration depths after mineralization among multiple groups, one-way analysis of variance (ANOVA) was performed, with pairwise comparisons between groups conducted using the LSD method. The significance level was set at $\alpha = 0.05$.

Results

Characterization of the Solutions by General View and FTIR

The freshly prepared PAMAM-COOH/ACMP and PAMAM-COOH/ACMP-MDP ethanol solutions were clear and colorless liquids without any precipitate (Figure 1A and C). After 60 days of storage at room temperature, they remained as clear and colorless liquids without precipitate (Figure 1B and D). The chemical bond characteristics of PAMAM-COOH/ACMP and PAMAM-COOH/ACMP-MDP were analyzed using FTIR. In the freshly configured solution (Figure 1E), the Raman peaks of PO_4^{3-} near 600 cm^{-1}, and 1080 cm^{-1} was observed in both groups, indicating the presence of ACP.[18] Additionally, the characteristic peaks of the amide bond (-NH-CO-) and carbonyl group (-C=O) in PAMAM-COOH were also observed near 1560 cm^{-1} and 1651 cm^{-1}. Moreover, PAMAM-COOH/ACMP-MDP exhibited a characteristic peak for the carbonyl group (-C=O) of MDP near 1730 cm^{-1}. In summary, the FTIR spectra of PAMAM-COOH/ACP-MDP presented the characteristic group of PAMAM-COOH (-C=O, -NH-CO-), ACP (PO_4^{3-}) and MDP (-C=O) simultaneously, indicating that it was a combination of PAMAM-COOH, ACP, and MDP. In the solution after 60 days of storage (Figure 1F), the characteristic group peaks of ACP, PAMAM-COOH and MDP were also present, indicating that the solution was chemically stable.

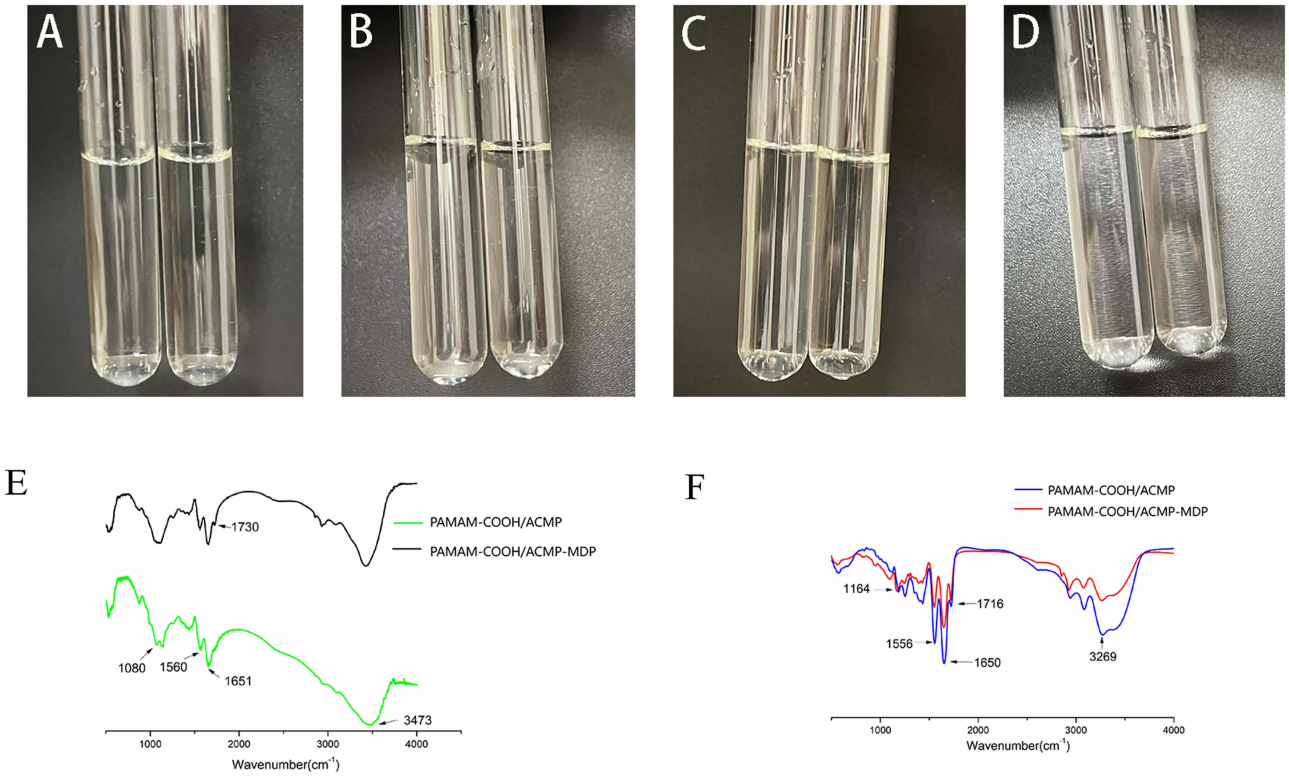

Figure 1 (**A-D**) General view of prepared solutions, the left test tubes was 50% ethanol solution as control. (**A,C**) fresh PAMAM-COOH/ACMP and PAMAM-COOH/ACMP-MDP. (**B,D**) PAMAM-COOH/ACMP and PAMAM-COOH/ACMP-MDP were stored for 60 days. The solutions were colorless clear liquid without precipitate. (**E**) FTIR analysis results of freshly prepared PAMAM-COOH/ACMP and PAMAM-COOH/ACMP-MDP. (**F**) FTIR analysis results of PAMAM-COOH/ACMP and PAMAM-COOH/ACMP-MDP after storage for 60 days.

https://doi.org/10.2147/IJN.S500283

Characterization of the Solutions by XRD

The phase characteristics of PAMAM-COOH/ACMP and PAMAM-COOH/ACMP-MDP were analyzed using XRD at a scanning rate of 0.02°/min across an incidence angle range of 0–100°. The XRD analysis of the fresh samples (Figure 2A) was basically consistent with that of the samples stored for 60 days (Figure 2B). The XRD patterns of PAMAM-COOH/ACMP and PAMAM-COOH/ACMP-MDP exhibited a distinct broad peak at 2θ = 24°, indicating the characteristic structure of amorphous phase materials. A peak at approximately 5° was observed in the XRD spectra of PAMAM-COOH/ACMP. This phenomenon may be attributed to the scattering peak of air, which can occasionally scatter around 5° during the process. Additionally, it is possible that the freshly prepared PAMAM-COOH/ACMP was not completely crystallized at the initial stage of its formation, leading to the observed scattering peaks. This suggests that

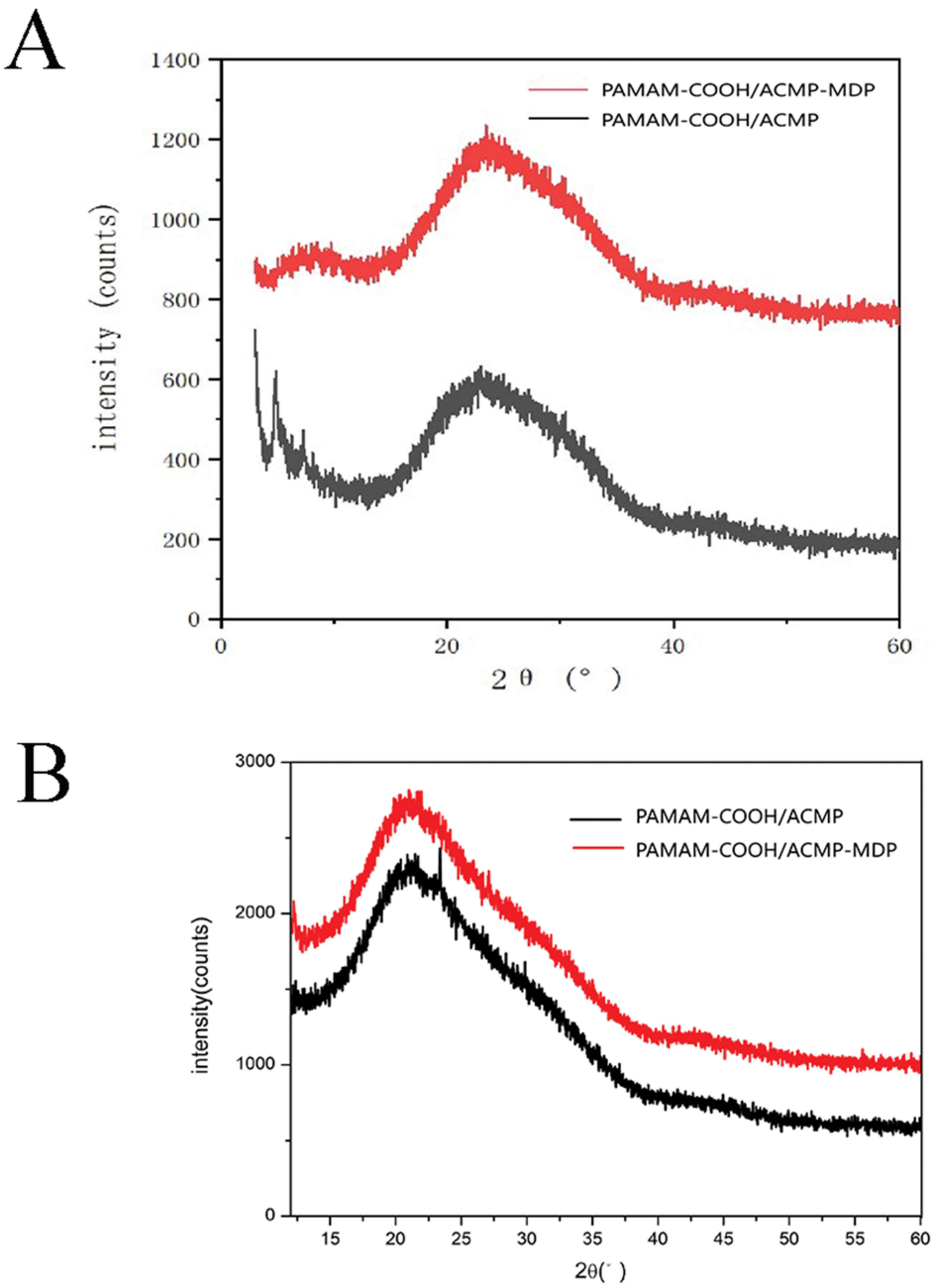

Figure 2 (**A**) XRD analysis results of freshly prepared PAMAM-COOH/ACMP and PAMAM-COOH/ACMP-MDP. (**B**) XRD analysis results of PAMAM-COOH/ACMP and PAMAM-COOH/ACMP-MDP after storage for 60 days. The independent large packet peak characteristic of amorphous phase material can be seen at 2θ=24°.

PAMAM-COOH/ACMP may exhibit some instability. These findings indicate that the PAMAM-COOH/ACMP-MDP we formulated can maintain an amorphous phase while demonstrating good stability.

Microscopic Morphology and Particle Size Analysis of the Remineralized Solutions

The microscopic morphological characteristics of PAMAM-COOH/ACMP and PAMAM-COOH/ACMP-MDP were observed using TEM. The particle diameters were calculated from the obtained TEM images. The PAMAM-COOH/ACMP particles (Figure 3A) exhibited almost circular shapes and good dispersion under TEM, but there was a slight tendency towards polymerization and non-uniform sizes. Conversely, the PAMAM-COOH/ACMP-MDP particles (Figure 3B) showed improved dispersion and more consistent particle sizes. After 60 days of storage, the solutions were retested and exhibited a similar circular particle structure to that of the newly prepared samples (Figure 3C and D), with high particle dispersion and no signs of agglomeration. Some numerous vacuoles were observed in both particle types because of the water within the particles readily vaporized when subjected to high-energy electron beams during electron microscopy, leading to the continuous development of vacuoles within the nanoparticles. This phenomenon suggested that these particles were non-solid mineral clusters. Furthermore, no diffraction spots or rings were detected in SAED analysis, indicating that these materials were amorphous substances (top right corner of Figure 3A–D).

The statistical analysis of particle sizes was performed, and the results were presented in Figure S3. The particles were grouped as freshly prepared PAMAM-COOH/ACMP (group A1) and PAMAM-COOH/ACMP-MDP (group B1), 60 days of storage PAMAM-COOH/ACMP (group A2) and PAMAM-COOH/ACMP-MDP (group B2). At high magnification, the particles revealed an average particle size of 81.97 ± 19.27 nm (group A1), 49.69 ± 6.47 nm (group B1), 59.73 ± 8.39 nm (group A2), 49.29 ± 9.44 nm (group B2). The particle size of the PAMAM-COOH/ACMP-MDP showed no significant change, whereas the PAMAM-COOH/ACMP exhibited a decreasing trend in particle size after this period. The decreasing trend may be due to the instability after the formation of PAMAM-COOH/ACMP, part of the groups were re-dissociated into ionic state after long-term preservation, which also indicated the doubts about the long-term stability of PAMAM-COOH/ACMP. Therefore, these results showed that the particle size of PAMAM-COOH/ACMP-MDP complex was significantly smaller than that of PAMAM-COOH/ACMP complex and more stable.

Elemental Analysis of the Remineralized Solutions

The solutions were analyzed using Scanning Transmission Electron Microscopy (STEM) coupled with Energy Dispersive X-Ray Spectroscopy (EDX) to confirm the composition of the particles. The PAMAM-COOH/ACMP and PAMAM-

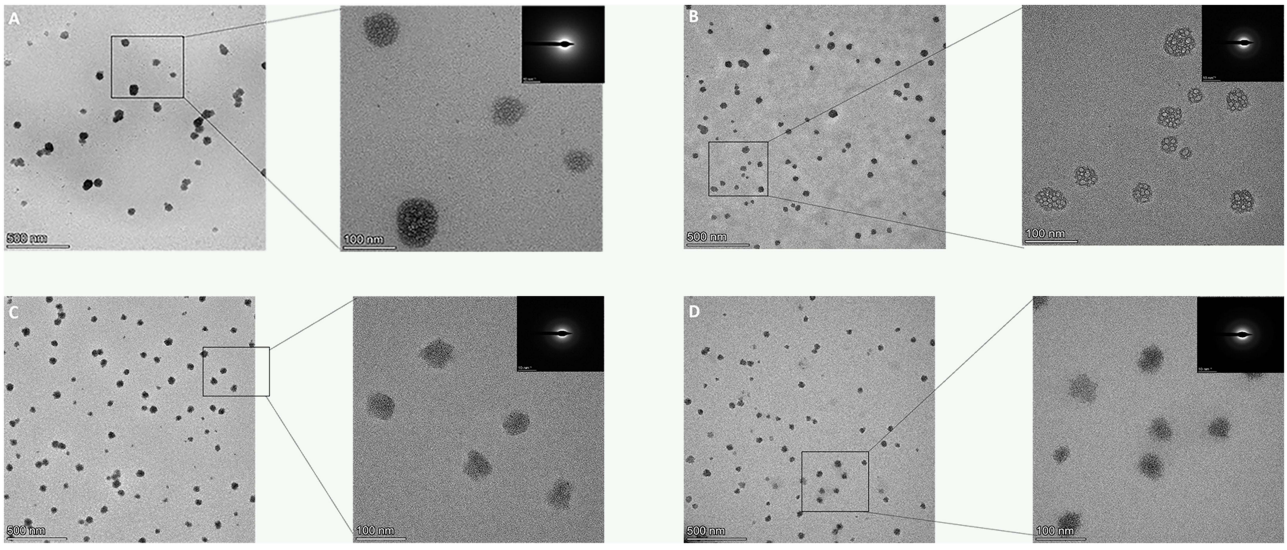

Figure 3 (**A,B**) TEM and SEAD observations of PAMAM-COOH/ACMP and PAMAM-COOH/ACMP-MDP. The particles were almost circular and dispersed well. No diffraction spots or rings were found in SEAD detection, indicating that they were all amorphous materials. (**C,D**) After 60 days of storage, similar round particle structure was present, with high particle dispersion and no agglomeration phenomenon. No diffraction spots or diffraction rings were found in SEAD detection.

https://doi.org/10.2147/IJN.S500283

COOH/ACMP-MDP particles were enriched with calcium (Ca) and phosphorus (P), confirming that they were clusters of Ca and P. Additionally, small amounts of magnesium (Mg) and nitrogen (N) were detected in the particles. Carbon was not listed due to its indistinguishability from the background, which was affected by air component interference (Figure 4). The results of the fresh configuration were largely consistent with those obtained after 60 days of storage, further demonstrating that the remineralization solution we prepared exhibited good dispersibility and maintained nanometer size with excellent stability.

The Remineralization of Partially Demineralized Human Dentin Tablets Surface

The remineralization of dentin tablet surfaces was observed using CLSM. To ensure comparability between groups, the CLSM observation parameters were consistently set for all samples. In the blank group, no remineralized deposits were detected on the surface or within the dentin tubules (Figure 5 A1 and A2). In the ACMP group, remineralized deposits were observed solely on the surface and in the superficial layer of the dentin tubules, with no deposits detected in the depths of the tubules (Figure 5 B1 and B2). The MDP group exhibited a small amount of fluorescence on the surface of the dentin tubules, which did not penetrate into the interiors, indicating that the fluorescence may represent only an attachment (Figure 5 C1 and C2). Fluorescence-labeled calcium ions were observed in the deep dentin tubules of both the PAMAM-COOH/ACMP group (Figure 5 D1 and D2) and the PAMAM-COOH/ACMP-MDP group (Figure 5 E1 and E2), with the fluorescence concentration in the PAMAM-COOH/ACMP-MDP group appearing to be higher. The depths of calcium ion infiltration into the dentin tubules across all groups were illustrated in Figure S4A. The blank and MDP groups were excluded from statistical analysis due to the absence of significant mineral deposition. The infiltration depths of the dentin tubules in the PAMAM-COOH/ACMP and PAMAM-COOH/ACMP-MDP groups were greater than that in the ACMP group (Figure S4B).

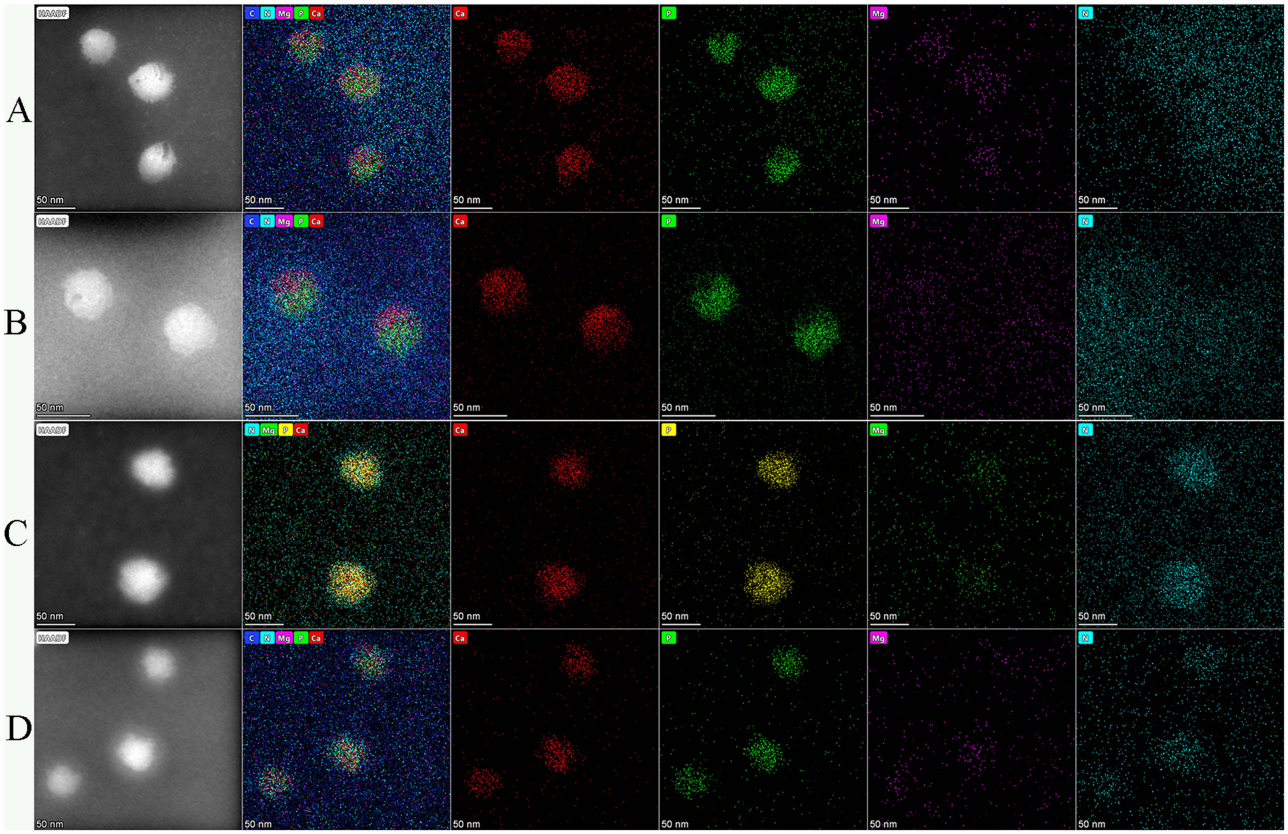

Figure 4 (**A,B**) Elemental analysis plots of freshly prepared PAMAM-COOH/ACMP and PAMAM-COOH/ACMP-MDP. The enrichment of calcium and phosphorus elements in the particles confirms that these particles were calcium and phosphorus clusters. (**C,D**) After 60 days of storage, the elemental composition of the particles were basically the same as that of fresh configuration, indicating the particles' well-dispersed and nano size stability.

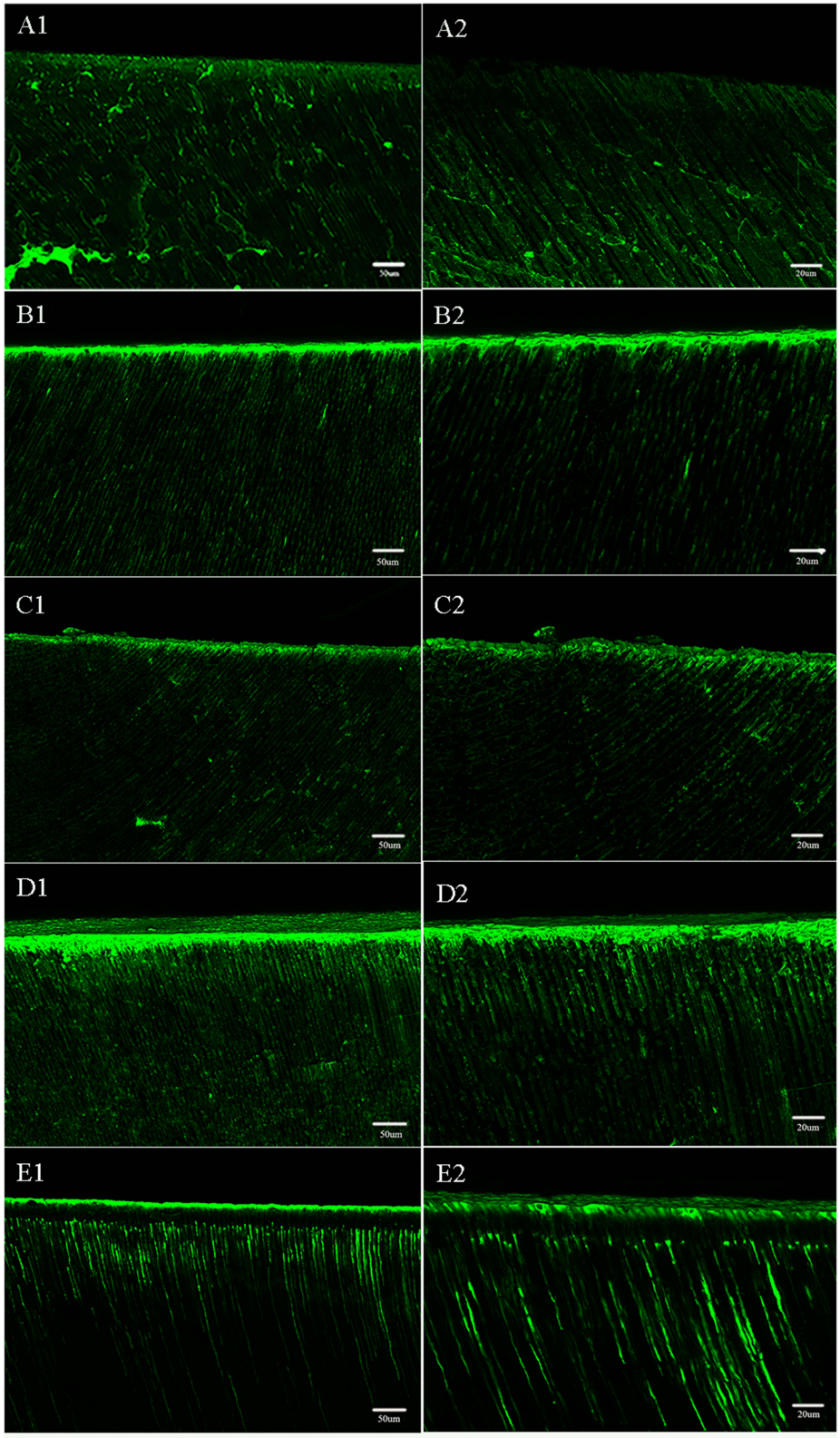

Figure 5 (A1,A2) the blank group. (B1,B2) the ACMP group. (C1,C2) the MDP group. (D1,D2) the PAMAM-COOH/ACMP group. (E1,E2) the PAMAM-COOH/ACMP-MDP group. Except the blank group and MDP group, new mineral deposits were observed on the surface and inside of the dentin tubules in other groups, and fluorescently labeled calcium ions in PAMAM-COOH/ACMP group and PAMAM-COOH/ACMP-MDP group could penetrate deep into the dentin tubules.

https://doi.org/10.2147/IJN.S500283

The Effect of Surface Remineralization of Completely Demineralized Human Dentin Tablets

We further observed the specific details of remineralization using SEM. In the blank group, collagen fibers were completely exposed, exhibiting finer fibers and larger interfiber spaces (Figure 6 A1-3). Compared to the blank group, the collagen fibers on the surface were thicker in ACMP group (Figure 6 B1-3), but the deep fibers remained noticeably loose with no significant mineralization. In the MDP group, collagen fibers on the surface of the dentin tubules were thickened and the space was reduced, but the deep fibers of the dentin tubules were not thickened and the space was reduced. The surface thickening may be due to the infiltration of MDP into the dentin tubules (Figure 6 C1-3). In the PAMAM-COOH/ACMP group (Figure 6 D1-3) and PAMAM-COOH/ACMP-MDP group (Figure 6 E1-3), distinct characteristics of collagen fiber mineralization were evident both on the surface and within the deep dentin tubules, the collagen fibers were thicker with reduced interfiber space. High-power microscopic observations of the same location in each group were presented in Figure S5. In both the PAMAM-COOH/ACMP and PAMAM-COOH/ACMP-MDP groups, segmental thickening of dentin collagen fibers was more pronounced, and the mineralized regions were interconnected.

TEM was also performed on the dentin tubules. Due to sectioning limitations, only deep dentin collagen fibers were observable. In the blank, ACMP, and MDP groups, no deeply stained mineral particles were detected within the deep dentin collagen fibers. In contrast, significant internal and external mineralization features of collagen fibers were observed in the peritubular dentin of the PAMAM-COOH/ACMP and PAMAM-COOH/ACMP-MDP groups (Figure 7 D1-2, E1-2). The characteristic periodic transverse lines of the collagen fibers were absent, and densely arranged deeply dyed mineral particles were aligned along the longitudinal axes of the fibers, with mineral deposits observable outside the fibers (Figure S6). These findings corroborate the previous results obtained from CLSM regarding the surface remineralization effects on partially demineralized human dentin specimens. The ACMP group was capable of mineralizing only the surface collagen fibers of the dentin but failed to penetrate into the deeper dentin to induce mineralization. In contrast, both the PAMAM-COOH/ACMP and PAMAM-COOH/ACMP-MDP groups successfully facilitated mineralization of collagen fibers within the deep dentin.

Discussion

In hard tissues, biomacromolecules such as chondroitin sulfate and DMP1 play a crucial role in the biomolecular mineralization of collagen, regulating the nucleation and growth of biomolecular proteins. During the crystal growth of biomaterials, including calcium phosphate, oxalate, and carbonate, proteins with carboxyl group sequences exhibit an inhibitory effect.[22–24] The carboxyl group is a key functional group influencing the crystallization and growth of HAP. In our previous research, we investigated the use of carboxyl-rich PAMAM-COOH to stabilize ACP, leading to the formation of the PAMAM-COOH/ACP nanocomplex.[17] This study addresses the limitations of the original ACP composites, to make it more stable and last for a long time. We developed a new ACP nanocomplex in an ethanol solution, PAMAM-COOH/ACMP-MDP, enabling its application in dentin bonding. FTIR and other analytical results confirmed the presence of PAMAM-COOH, ACP and MDP in the complex particles, indicating that the particles were indeed the PAMAM-COOH/ACMP-MDP complex.

In this study, in addition to PAMAM-COOH, the introduction of Mg^{2+} was another key measure to stabilize ACP. Mg^{2+} plays a vital role in the formation and mineralization of hydroxyapatite in human dentin.[25] It has a notable stabilizing effect on ACP,[26] significantly prolonging the induction time for the conversion of ACP to HAP, a process that is dependent on the concentration of Mg^{2+}.[17,27] Based on the findings of previous studies, we determined the optimal calcium-to-magnesium ratio in the solution, achieving effective stabilization of ACP. Both PAMAM-COOH/ACMP and PAMAM-COOH/ACMP-MDP ethanol solution avoided the phenomenon of polymerization, and maintained good dispersibility after 60 days of storage at room temperature. However, compared with 60 days ago, the particle size of PAMAM-COOH/ACMP had a decreasing trend, indicating that its long-term stability was still doubtful. There was no significant difference in particle size between PAMAM-COOH/ACMP-MDP group and 60 days ago. Therefore, the complex showed good storage performance, which is of great significance for future clinical applications.

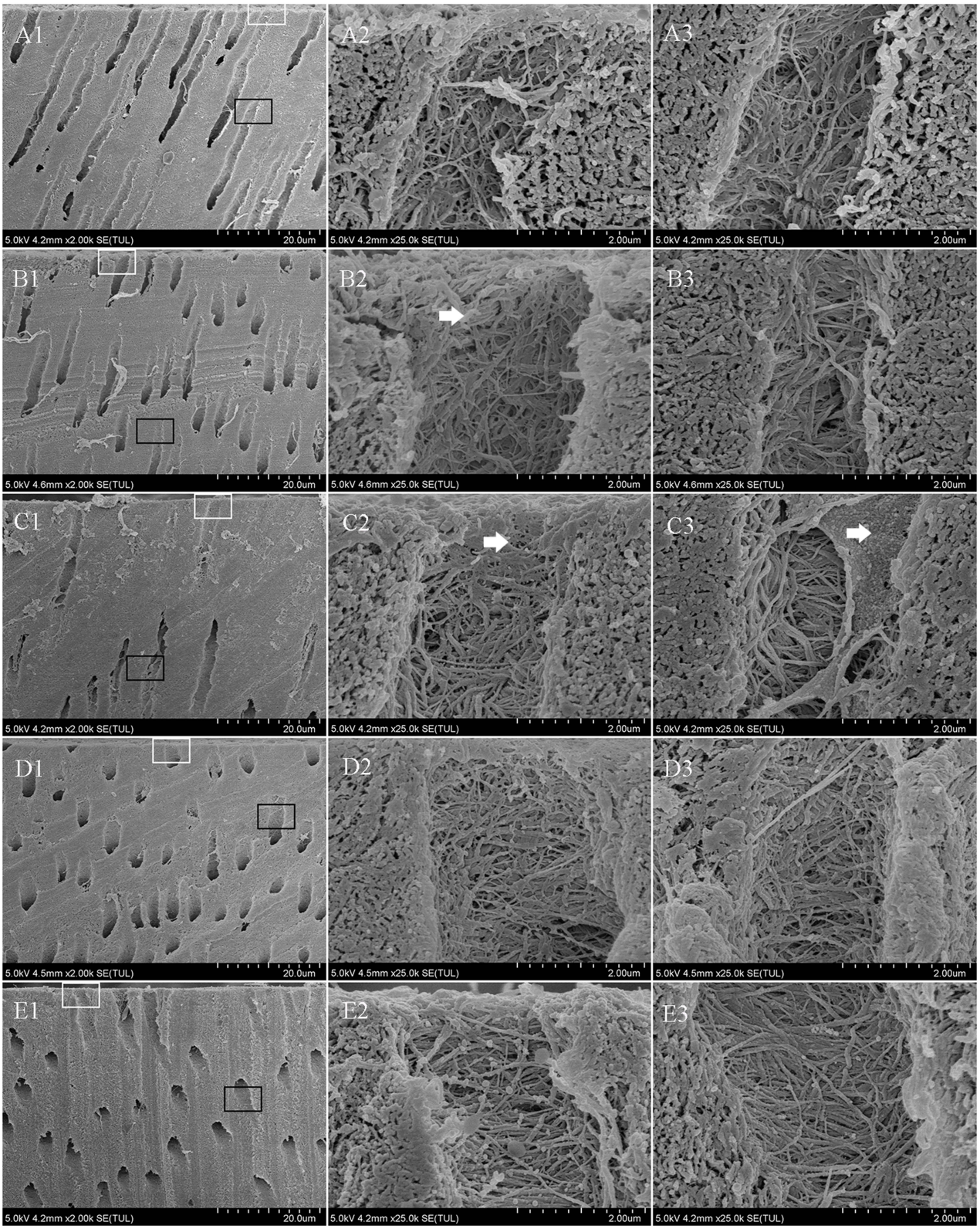

Figure 6 The images in the left column were all low-power field of view (×2000), and the white box selection in the left column was enlarged (×25000) in the middle column, and the black box selection in the left column was enlarged (×25000) in the right column. (A1-A3) the blank group, the fibers were finer and the gap was larger. (B1-B3) the ACMP group, mineralization was limited to the surface layer of the collagen web (arrow), but the deep tubule mineralization was not obvious (B3). (C1-C3) the MDP group, a membrane-like adhesive layer appeared on the surface of the surface collagen fiber network (arrow), and the collagen fiber network below the membrane-like layer showed no mineralization. (D1-D3) the PAMAM-COOH/ACMP group, (E1-E3) the PAMAM-COOH/ACMP-MDP group, In these two groups, obvious characteristics of collagen fiber mineralization could be seen both on the surface and deep dentin tubules.

https://doi.org/10.2147/IJN.S500283

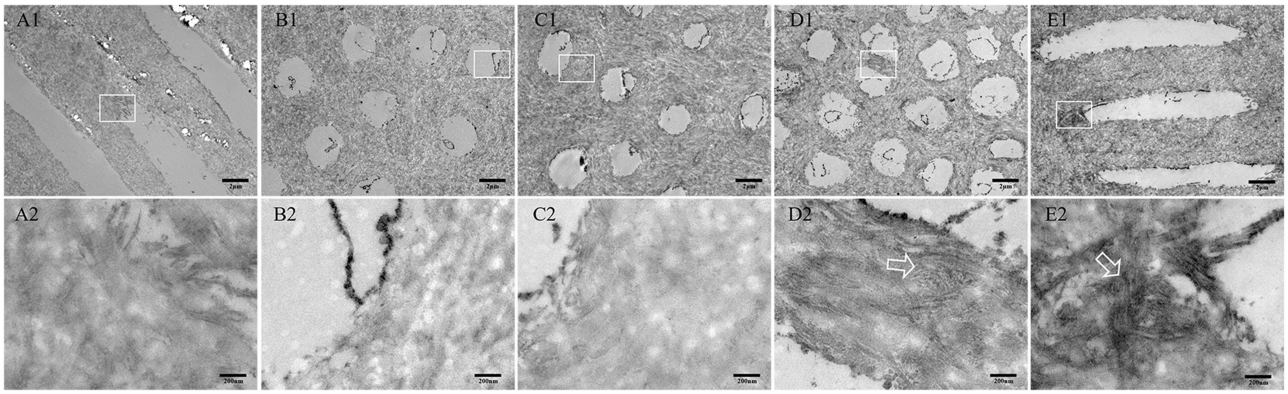

Figure 7 (A1,A2) the blank group. (B1,B2) the ACMP group. (C1,C2) the MDP group. (D1,D2) the PAMAM-COOH/ACMP group. (E1,E2) the PAMAM-COOH/ACMP-MDP group. The ascending images were all low-power field of view (×3000), and the white box selection of the descending images was enlarged. In the blank group, ACMP group and MDP group, there were no deeply stained mineral particles in the collagen fibers, while the periductal dentin of PAMAM-COOH/ACMP group and PAMAM-COOH/ACMP-MDP group showed obvious characteristics of both internal and external mineralization of collagen fibers. Deeply stained mineral particles can be seen in the fibers in dense longitudinal arrangement along the fibers (arrow).

MDP was incorporated in this study due to its long hydrophobic spacer chain, which allows it to stably bind to calcium salts.[28] When the phosphate group of MDP was attached to ACP, the hydrophobic spacer chain was positioned laterally, enhancing the stability of the complex in organic solutions. The results of this experiment demonstrated that the particle size of the PAMAM-COOH/ACMP-MDP complex in ethanol solution was significantly smaller and more homogeneous. The ACP complex retains a very small nanometer size, and since the ACP complex particles consist of amorphous calcium phosphate clusters, they possess the ability to infiltrate collagen fibers, thereby creating conditions conducive to the mineralization of collagen fibers.

Biomimetic mineralization of collagen fibers that promotes demineralization represents a highly promising approach for protecting hybrid layers at dentin bonding interfaces. The mechanism of fiber mineralization induced by the polymer PAMAM-COOH used in this study may be similar to that of the macromolecular brush polymer used in a study by Yu, who synthesized carboxyl-rich carboxyl-polyethylene glycol terpolymer (PEG-COOH; 42 kDa) and polyethylene glycol/polyacrylic acid copolymer (PEG-PAA; 44 kDa) has been shown to induce mineralization in collagen fibre.[29] It has also been shown that polymers rich in carboxyl groups can effectively induce biomimetic mineralization of collagen fibers.[30–32] Based on these findings, we speculate that the carboxyl groups rich in PAMAM-COOH may play a key role in inducing fiber mineralization, which is consistent with our current findings. In this experiment, except for the blank group and the MDP group, the remaining three groups were able to remineralize the demineralized dentin. Notably, the PAMAM-COOH/ACMP group and the PAMAM-COOH/ACMP-MDP group exhibited exceptional remineralization capabilities, not only remineralizing the demineralized layer but also penetrating into the deeper dentin tubules. This may prove advantageous in future clinical bonding applications by sealing dentinal tubules with calcification, thereby preventing fluid infiltration into the adhesive interface and subsequent failure.

According to the size exclusion theory of collagen fiber mineralization,[33] molecules smaller than 6 kDa can enter the interior of the fibers, while those larger than 40 kDa are excluded. Our results indicated that the average particle size of the PAMAM-COOH/ACMP group was larger than that of the PAMAM-COOH/ACMP-MDP group; however, both groups exhibited a similar capacity to induce collagen fiber mineralization, highlighting the limitations of the size exclusion theory in this context. According to the non-classical nucleation theory, calcium-phosphorus ions formed during the early stages of mineralization preassemble into relatively stable nano-liquid ACP, referred to as Polymer-induced liquid-precursor (PILP). This ACP can penetrate the interior of collagen fibers through capillary action or Gibbs-Donnan equilibrium,[8,34] subsequently converting into HAP crystals via a dissolution-recrystallization mechanism. Our results showed that both PAMAM-COOH/ACMP-MDP and PAMAM-COOH/ACMP were amorphous calcium phosphate clusters, belonging to the PILP category. In the context of PILP theory, ACPs can be drawn into the inner space of

collagen fibrils due to their fluid properties.[35,36] This theory may reasonably explain why ACP composites with different particle sizes can effectively induce collagen fiber remineralization in the present study.

In addition, according to the Gibbs-Donnan equilibrium theory,[34] the charge distribution and osmotic pressure between the water chamber outside the fiber and the interior of the fiber were responsible for collagen mineralization in the polyelectrolyte collagen mineralization system. In this study, we hypothesized that the balance of electrostatic forces generated by electrostatic neutrality between the negatively charged PAMAM-COOH and positively charged regions,[37] along with the high osmotic pressure between the inner and outer fiber interstices, may drive the infiltration of ACP and calcium ions into the collagen fibrils, thereby promoting mineralization within the fibers. The high osmotic pressure could potentially result from the coordination between PAMAM-COOH and magnesium ions, which supports the maintenance of the amorphous phase of ACP. This coordinated action inhibited the rapid crystallization of ACP and the subsequent depletion of calcium ions outside the fiber, thereby ensuring the supersaturation of calcium ions in the external environment. This also indicates that ACP stabilizers play a crucial role in the mineralization process of collagen fibers. Our results showed that PAMAM-COOH/ACMP-MDP ethanol solution could stabilize ACP and induced the mineralization of demineralized dentine collagen fibers. While direct observation of intrafibrillary mineralization in dentin through experiments remains unfeasible, a more critical focus lies on the role of PAMAM-COOH/ACMP-MDP in dentin bonding restoration, as well as its potential future applications in clinical practice. This aspect represents both the direction and goal of our ongoing research.

Conclusion

Based on the current experimental results and within the limits of this study, we successfully synthesized a new PAMAM-COOH/ACMP-MDP ethanol solution by combining carboxyl-rich PAMAM-COOH, magnesium ions, and MDP. The physical and chemical properties of the solution were stable and could be preserved for a long time. It can promote the remineralization of demineralized dentin by stabilizing ACP and meet the necessary conditions of bionic mineralization of the interface between demineralized collagen fiber and resin. The findings suggest its potential application in caries treatment and adhesive repair, providing a new foundation for improved filling repair treatments and the design and development of innovative adhesives.

Data Sharing Statement

The datasets used and/or analyzed during the current study are available from the corresponding author on reasonable request.

Ethics Approval and Consent to Participate

The Guangxi Medical University Ethics Committee's guiding principles (Protocol Number: 20220026) were followed in all experiments. Our study complied with the Declaration of Helsinki.

Author Contributions

All authors made a significant contribution to the work reported, whether that is in the conception, study design, execution, acquisition of data, analysis, and interpretation, or all these areas; took part in drafting, revising or critically reviewing the article; gave final approval of the version to be published; have agreed on the journal to which the article has been submitted; and agree to be accountable for all aspects of the work.

Funding

This work was supported by the National Natural Science Foundation of China (grant no. 82260190) and the Nanning Qingxiu District Science and Technology Program (grant no. 2021008).

Disclosure

The authors report no conflicts of interest in this work.

References

1. Liu Y, Kim YK, Dai L, et al. Hierarchical and non-hierarchical mineralisation of collagen. *Biomaterials*. 2011;32(5):1291–1300. doi:10.1016/j.biomaterials.2010.10.018
2. Breschi L, Martin P, Mazzoni A, et al. Use of a specific MMP-inhibitor (galardin) for preservation of hybrid layer. *Dental Materials*. 2010;26(6):571–578. doi:10.1016/j.dental.2010.02.007
3. Su M, Yao S, Gu L, Huang Z, Mai S. Antibacterial effect and bond strength of a modified dental adhesive containing the peptide nisin. *Peptides*. 2018;99:189–194. doi:10.1016/j.peptides.2017.10.003
4. Chrysanthakopoulos NA. Placement, replacement and longevity of composite resin-based restorations in permanent teeth in Greece. *Int Dental J*. 2012;62(3):161–166. doi:10.1111/j.1875-595X.2012.00112.x
5. Drummond JL. Degradation, fatigue, and failure of resin dental composite materials. *J Dent Res*. 2008;87(8):710–719. doi:10.1177/154405910808700802
6. Breschi L, Mazzoni A, Ruggeri A, Cadenaro M, Di Lenarda R, De Stefano Dorigo E. Dental adhesion review: aging and stability of the bonded interface. *Dental Materials*. 2008;24(1):90–101. doi:10.1016/j.dental.2007.02.009
7. Yao S, Xu Y, Shao C, Nudelman F, Sommerdijk N, Tang R. A biomimetic model for mineralization of type-i collagen fibrils. *Methods mol Biol*. 2019;1944:39–54.
8. Olszta MJ, Cheng X, Jee SS, et al. Bone structure and formation: a new perspective. *Mater Sci Eng R Rep*. 2007;58(3–5):77–116. doi:10.1016/j.mser.2007.05.001
9. Gajjeraman S, Narayanan K, Hao J, Qin C, George A. Matrix macromolecules in hard tissues control the nucleation and hierarchical assembly of hydroxyapatite. *J Biol Chem*. 2007;282(2):1193–1204. doi:10.1074/jbc.M604732200
10. Liu Y, Li N, Qi YP, et al. Intrafibrillar collagen mineralization produced by biomimetic hierarchical nanoapatite assembly. *Adv Materials*. 2011;23(8):975–980. doi:10.1002/adma.201003882
11. Moradian-Oldak J, George A. Biomineralization of enamel and dentin mediated by matrix proteins. *J Dent Res*. 2021;100(10):1020–1029. doi:10.1177/00220345211018405
12. Landis WJ, Silver FH. Mineral deposition in the extracellular matrices of vertebrate tissues: identification of possible apatite nucleation sites on type I collagen. *Cells Tissues Organs*. 2009;189(1–4):20–24. doi:10.1159/000151454
13. Jee SE, Zhou J, Tan J, et al. Investigation of ethanol infiltration into demineralized dentin collagen fibrils using molecular dynamics simulations. *Acta Biomater.* 2016;36:175–185. doi:10.1016/j.actbio.2016.03.012
14. Tsiourvas D, Tsetsekou A, Kammenou MI, Boukos N. Controlling the Formation of Hydroxyapatite Nanorods with Dendrimers. *J Am Ceram Soc*. 2011;94(7):2023–2029. doi:10.1111/j.1551-2916.2010.04342.x
15. Yang X, Shang H, Ding C, Li J. Recent developments and applications of bioinspired dendritic polymers. *Polym Chem*. 2015;6(5):668–680. doi:10.1039/C4PY01537A
16. Lin X, Xie F, Ma X, Hao Y, Qin H, Long J. Fabrication and characterization of dendrimer-functionalized nano-hydroxyapatite and its application in dentin tubule occlusion. *J biomater sci Poly ed*. 2017;28(9):846–863. doi:10.1080/09205063.2017.1308654
17. Yang J, Huang J, Qin H, Long J, Lin X, Xie F. Remineralization of human dentin type I collagen fibrils induced by carboxylated polyamidoamine dendrimer/amorphous calcium phosphate nanocomposite: an in vitro study. *J biomater sci Poly ed*. 2021;33(5):668–686. doi:10.1080/09205063.2021.2008789
18. Xie H, Sun J, Xie F, He S. Intrafibrillar mineralization of type I collagen by micelle-loaded amorphous calcium phosphate nanoparticles. *RSC Adv.* 2023;13(17):11733–11741. doi:10.1039/D3RA01321A
19. Yoshioka M, Yoshida Y, Inoue S, et al. Adhesion/decalcification mechanisms of acid interactions with human hard tissues. *J Biomed Mater Res*. 2002;59(1):56–62. doi:10.1002/jbm.1216
20. Fu B, Sun X, Qian W, Shen Y, Chen R, Hannig M. Evidence of chemical bonding to hydroxyapatite by phosphoric acid esters. *Biomaterials*. 2005;26(25):5104–5110. doi:10.1016/j.biomaterials.2005.01.035
21. Gelli R, Scudero M, Gigli L, et al. Effect of pH and Mg(2+) on Amorphous Magnesium-Calcium Phosphate (AMCP) stability. *J Colloid Interface Sci*. 2018;531:681–692. doi:10.1016/j.jcis.2018.07.102
22. Fujisawa R, Wada Y, Nodasaka Y, Kuboki Y. Acidic amino acid-rich sequences as binding sites of osteonectin to hydroxyapatite crystals. *BBA*. 1996;1292(1):53–60. doi:10.1016/0167-4838(95)00190-5
23. Wesson JA, Worcester E. Formation of hydrated calcium oxalates in the presence of poly-L-aspartic acid. *Scanning Microsc*. 1996;10(2):415–423;423–414.
24. van der Reijden WA, Buijs MJ, Damen JJ, Veerman EC, ten Cate JM, Nieuw Amerongen AV. Influence of polymers for use in saliva substitutes on de- and remineralization of enamel in vitro. *Caries Res*. 1997;31(3):216–223. doi:10.1159/000262403
25. Bertran O, Del Valle LJ, Revilla-López G, et al. Synergistic approach to elucidate the incorporation of magnesium ions into hydroxyapatite. *Chemistry.* 2015;21(6):2537–2546. doi:10.1002/chem.201405428
26. Eanes ED, Posner AS. Intermediate phases in the basic solution preparation of alkaline earth phosphates. *Calcif Tissue Res*. 1968;2(1):38–48. doi:10.1007/BF02279192
27. Pa BAL, Posner AS. Magnesium stabilization of amorphous calcium phosphate A kinetic study. *Mate Res Bull*. 1974;9(7):907–9163. doi:10.1016/0025-5408(74)90169-X
28. Yoshihara K, Yoshida Y, Hayakawa S, et al. Nanolayering of phosphoric acid ester monomer on enamel and dentin. *Acta Biomater.* 2011;7(8):3187–3195. doi:10.1016/j.actbio.2011.04.026
29. Lmi Y, Kasi RM, Kasi RM, et al. Enhanced intrafibrillar mineralization of collagen fibrils induced by brushlike polymers. *ACS Appl. Mater. Interfaces*. 2018;10(34):28440–28449. doi:10.1021/acsami.8b10234
30. Wu S, Gu L, Huang Z, et al. Intrafibrillar mineralization of polyacrylic acid-bound collagen fibrils using a two-dimensional collagen model and Portland cement-based resins. *Eur J Oral Sci*. 2017;125(1):72–80. doi:10.1111/eos.12319
31. Wei S, Wu H, Luo XJ. Biomineralization precursor carrier system based on carboxyl-functionalized large pore mesoporous silica nanoparticles. *Curr Med Sci*. 2020;40(1):155–167. doi:10.1007/s11596-020-2159-3

32. Du T, Niu X, Hou S, Li Z, Li P, Fan Y. Apatite minerals derived from collagen phosphorylation modification induce the hierarchical intrafibrillar mineralization of collagen fibers. *J Biomed Mater Res Part A*. 2019;107(11):2403–2413. doi:10.1002/jbm.a.36747
33. Toroian D, Lim JE, Price PA. The size exclusion characteristics of type I collagen: implications for the role of noncollagenous bone constituents in mineralization. *J Biol Chem*. 2007;282(31):22437–22447. doi:10.1074/jbc.M700591200
34. Niu LN, Jee SE, Jiao K, et al. Collagen intrafibrillar mineralization as a result of the balance between osmotic equilibrium and electroneutrality. *Nature Mater*. 2017;16(3):370–378. doi:10.1038/nmat4789
35. Jee SS, Kasinath RK, DiMasi E, Kim -Y-Y, Gower L. Oriented hydroxyapatite in Turkey tendon mineralized via the polymer-induced liquid-precursor (PILP) process. *CrystEngComm*. 2011;13(6):2077. doi:10.1039/c0ce00605j
36. Jee SS, Culver L, Li Y, Douglas EP, Gower LB. Biomimetic mineralization of collagen via an enzyme-aided PILP process. *Journal of Crystal Growth*. 2010;312(8):1249–1256. doi:10.1016/j.jcrysgro.2009.11.010
37. Li J, Yang J, Li J, et al. Bioinspired intrafibrillar mineralization of human dentine by PAMAM dendrimer. *Biomaterials*. 2013;34(28):6738–6747. doi:10.1016/j.biomaterials.2013.05.046